Engineering Transactions, **70**(4): 373–390, 2022, doi: 10.24423/EngTrans.2238.20221125
Institute of Fundamental Technological Research Polish Academy of Sciences (IPPT PAN)
Université de Lorraine • Poznan University of Technology

Research Paper

Bending of a Stepped Sandwich Beam: The Shear Effect

Joanna KUSTOSZ*, Krzysztof MAGNUCKI, Damian GOLIWĄS

Łukasiewicz Research Network – Poznan Institute of Technology, Rail Vehicles Center
Poznań, Poland; e-mail: krzysztof.magnucki@pit.lukasiewicz.gov.pl,
damian.goliwas@pit.lukasiewicz.gov.pl

*Corresponding Author e-mail: joanna.kustosz@pit.lukasiewicz.gov.pl

This paper is devoted to the stepped sandwich beam with clamped ends subjected to a uniformly distributed load. The bending problem of the beam is formulated and solved with consideration of the classical sandwich beam of constant face thickness. Two differential equations of equilibrium based on the principle of the stationary potential energy of the classical beam are obtained and analytically solved. Moreover, numerical-FEM models of the beams are developed. Deflections for an exemplary beam family with the use of two methods are calculated. The results of the study are presented in figures and tables.

Keywords: stepped sandwich beam; clamped ends; shear effect; bending.

1. Introduction

Sandwich constructions, initiated in the mid-twentieth century, are the subject of contemporary studies and are intensively improved.

Noor *et al.* [15] reviewed 800 references devoted to computational models of sandwich plates and shells. Their review includes numerical results of thermally stressed sandwich panels. In addition, the authors cited 559 articles as complementary sources of information. Vinson [20] reviewed the possible applications of sandwich structures and discussed the basics of the structural mechanics of these structures. This revision contains 174 references. Icardi [5] developed a sublaminate model of a laminated or sandwiched beam based on the zig-zag theory. For this purpose, the author compared four models with linear or cubic approximation and with or without the zig-zag theory. The author described the advantages of higher-order displacement approximations in layers of sandwich or laminated structures, and proposed a model that can be used to calculate sandwich or laminate structures in which laminates are thick and whose material properties change in the layers. Steeves and Fleck [19] considered the three-point bending of sandwich beams made of composite faces and a polymer foam core. The authors focused on defining the collapse mode of this structure in relation to its geometry and weight. In addition, the authors compared the collapse strength of sandwich beams made of composite faces and a polymer core with those with a metal core and metal faces. A higher-order impact model of a sandwich beam with a soft core was presented by Yang and Qiao [23]. The authors considered the free vibrations of the sandwich beams impacted by a foreign object and compared these results with the numerical results. The model developed by Yang and Qiao can be used to design anti-impact sandwich structures. Magnucka-Blandzi and Magnucki [7] described the bending of a simply supported sandwich beam with a metal foam core. The authors formulated and solved a system of equations of equilibrium based on the theory of potential energy minimum. A numerical solution has also been presented. Carrera and Brischetto [2] reviewed the bending and vibration of sandwich plates and presented various theories: classical, higher-order, zig-zag, layerwise and mixed. Moreover, in their article, the authors considered benchmark problems of simply supported orthotropic panels. Carrera and Brischetto pointed out the sources of errors related to the ratio of length-to-thickness and the ratio of face-to-core-stiffness. Nguyen *et al.* [14] investigated the advantages of sandwich panels with stepped faces. The authors described many examples to prove that stepped facings can locally improve the strength and stiffness of sandwich structures. Kreja [6] reviewed the theoretical model of sandwich beams and their numerical implementation. The result of analyzing over 200 references is the fact that there is no universal numerical model for layered composite and sandwich panels. Wang *et al.* [21] described sandwich beams with metal facings and a core made of shape memory polymers. The authors considered two types of beams that differ from the material of facings (aluminum or steel). Xiaohui *et al.* [22] developed a higher-order broken line theory for laminated composite and sandwich structures, which is independent of the number of layers. Results of numerical studies have been presented by the authors. Phan *et al.* [16] developed a one-dimensional high-order theory for sandwich beams that are orthotropic and elastic. This theory is an extension of the high-order theory of sandwich beams and is based on three generalized coordinates in the core. The advantage of this approach is that it can be used to analyze sandwich beams, the core and faces made of any material. Moreover, the authors presented a detailed numerical analysis of this theory. The bending and buckling of a five- layer sandwich beam, in which a thin layer of glue bonds faces and a core, was described by Magnucki *et al.* [9]. In the article, the authors compared the analytical, numerical and experimental results of bending a five-layer sandwich beam. Sayyad and Ghugal [17] reviewed the bending, buckling and free vibration of sandwich beams and laminated composite. The authors also considered numerical modeling of laminated and sandwich structures. The review was made based on 515 references.

Magnucka-Blandzi [8] developed an analytical model of seven-layer beams with a corrugated core and three-layer facings and compared it with classic three-layer beams. An analytical model of this structure was formulated, taking into account the deformation depending on displacements and deformation fields as well as the rigidities of the layers. Moreover, Magnucka-Blandzi presented and compared the solution of equilibrium equations of a three- and seven-layer sandwich beam. Birman and Kardomateas [1] reviewed mathematical models, methods of analysis and problems in the design of sandwich structures. Their paper focused on novel works of sandwich structures and older articles were only mentioned as the basic sources of knowledge. The authors described different designs of sandwich structures, such as miscellaneous cores, nanotubes, smart materials and functionally graded. Furthermore, possible applications of sandwich structures in, for instance, aerospace, civil and marine engineering were presented. Sayyad and Ghugal [18] reviewed the analytical and numerical methods for modeling functionally graded sandwich beams using the theory of elasticity. Their article contains 250 citations and references. Furthermore, the authors suggested possible areas of further research on functionally graded sandwich structures. Magnucki *et al.* [10] developed a mathematical model of an unsymmetrical sandwich beam whose faces differ in thickness and mechanical properties. In the article, a mathematical model of the beam was formulated on the basis of broken-line hypothesis. The authors compared analytical results with solutions from two different FEM systems. The bending of simply supported sandwich beams and I-beams of symmetrical structure in two different load cases was considered by Magnucki [11]. The author developed two models based on zig-zag and nonlinear theory, respectively. The results of the analytical solution of equations of equilibrium for two load cases based on the total potential energy principle were presented.

A proposal for a general mathematical model of sandwich structures was presented by Magnucki and Magnucka-Blandzi [12]. This analytical model was thoroughly presented by the authors for the rectangular plate. Moreover, a system of plate equilibrium equations, which was formulated on the basis of the total potential energy principle, was solved. Chinh *et al.* [3] investigated the point interpolation meshfree method based on a polynomial basic function. This function is used for constructing shape functions and approximating displacement field of the computational domain. Moreover, the authors derived equilibrium equations of functionally graded sandwich beams from the principle of virtual work. The accuracy of the developed method was proved by comparison with results in literature. Drache *et al.* [4] developed the higher-order theory of shear and normal deformation of functionally graded sandwich beams. The novelty of this theory is that the hyperbolic cosine distribution of transverse shear stress has been explained. The authors presented the solution of equilibrium equations derived from the principle of virtual work. Results have been compared with the solutions in the literature. Magnucki *et al.* [13] presented a comparison of the bending, buckling and free flexural vibration of three models of a sandwich beam. The authors developed two shear theories of the deformation of a sandwich beam's cross-section. Furthermore, equations of motion for the presented models were formulated.

The subject of this study are the stepped sandwich beams with clamped ends of length L, total depth h, and width b. These beams are under a uniformly distributed load of intensity q (Fig. 1), and are placed in the Cartesian coordinate system xyz.

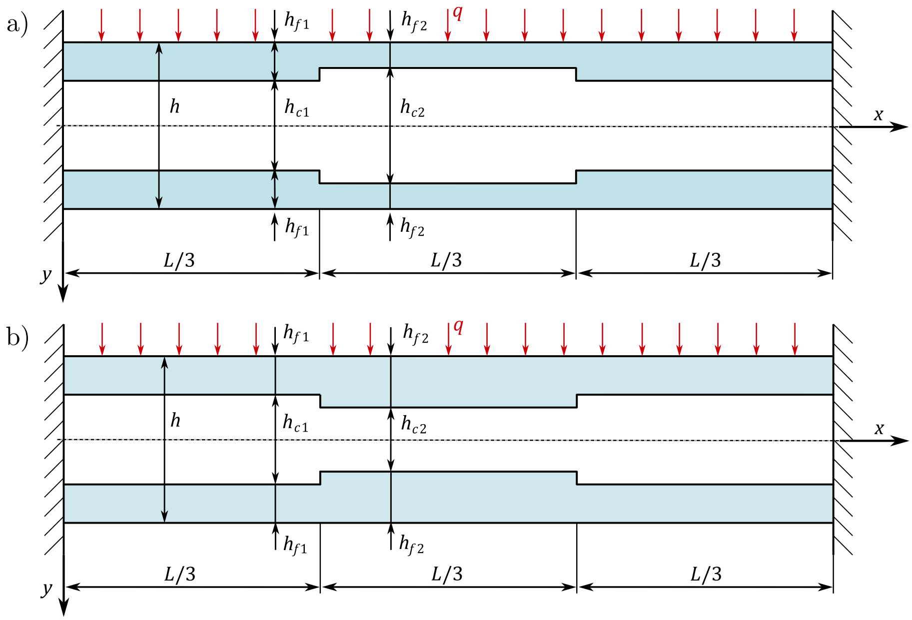

Fig. 1. Schemes of two cases of the stepped sandwich beam with clamped ends: a) thinner facings of the middle beam part ($h_{f2} \leq h_{f1}$), b) thicker facings of the middle beam part ($h_{f1} \leq h_{f2}$).

The paper's main goal is to elaborate analytical and numerical FEM models of this beam and determine deflections for sample beams.

2. Analytical model of the stepped sandwich beam and calculations

The deformation of a planar cross-section (a straight normal line) of the sandwich beam of constant faces' thickness with consideration of the "broken line" theory – classical model, presented, e.g., in [13], is shown in Fig. 2.

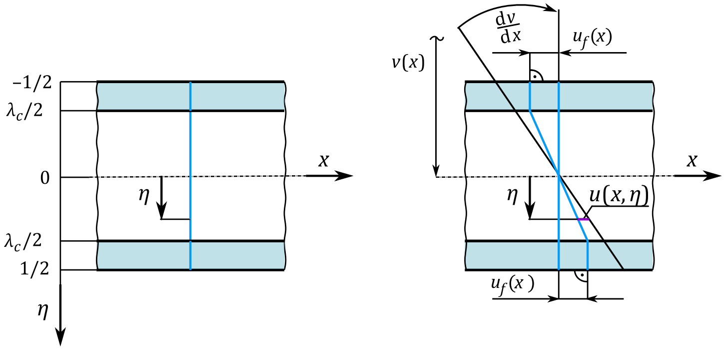

FIG. 2. Scheme of the deformation of a planar cross-section of the classical sandwich beam.

Based on the above scheme, the longitudinal displacements in the x-direction are as follows:

- the upper face $(-1/2 \leq \eta \leq -\chi_c/2)$

$$u(x,\eta) = -h\left[\eta\frac{\mathrm{d}v}{\mathrm{d}x} + \psi_f(x)\right], \tag{2.1}$$

- the core $(-\chi_c/2 \leq \eta \leq \chi_c/2)$

$$u(x,\eta) = -h\eta\left[\frac{\mathrm{d}v}{\mathrm{d}x} - \frac{2}{\chi_c}\psi_f(x)\right], \tag{2.2}$$

- the lower face $(\chi_c/2 \leq \eta \leq 1/2)$

$$u(x,\eta) = -h\left[\eta\frac{\mathrm{d}v}{\mathrm{d}x} - \psi_f(x)\right], \tag{2.3}$$

where $\eta = y/h$ is the dimensionless coordinate, $\psi_f(x) = u_f(x)/h$ is the dimensionless displacement function, $\chi_c = h_c/h$ is the relative thickness of the core, and $v(x)$ is the deflection of the beam.

Thus, the strains in particular layers are as follows:

- the upper face

$$\begin{aligned}
\varepsilon_x^{(uf)}(x,\eta) &= \frac{\partial u}{\partial x} = -h\left[\eta\frac{\mathrm{d}^2v}{\mathrm{d}x^2} + \frac{\mathrm{d}\psi_f}{\mathrm{d}x}\right], \\
\gamma_{xy}^{(uf)}(x,\eta) &= \frac{\partial u}{h\partial\eta} + \frac{\mathrm{d}v}{\mathrm{d}x} = 0,
\end{aligned} \tag{2.4}$$

- the core

$$\varepsilon_x^{(c)}(x,\eta) = -h\eta\left[\frac{\mathrm{d}^2 v}{\mathrm{d}x^2} - \frac{2}{\chi_c}\frac{\mathrm{d}\psi_f}{\mathrm{d}x}\right],$$
(2.5)
$$\gamma_{xy}^{(c)}(x) = \frac{\partial u}{h\partial\eta} + \frac{\mathrm{d}v}{\mathrm{d}x} = \frac{2}{\chi_c}\psi_f(x),$$

- the lower face

$$\varepsilon_x^{(lf)}(x,\eta) = \frac{\partial u}{\partial x} = -h\left[\eta\frac{\mathrm{d}^2 v}{\mathrm{d}x^2} - \frac{\mathrm{d}\psi_f}{\mathrm{d}x}\right],$$
(2.6)
$$\gamma_{xy}^{(lf)}(x,\eta) = \frac{\partial u}{h\partial\eta} + \frac{\mathrm{d}v}{\mathrm{d}x} = 0.$$

Consequently, the stresses in accordance with Hooke's law are in the following form:

- the upper/lower faces

$$\sigma_x^{(uf)}(x,\eta) = E_f\varepsilon_x^{(uf)}(x,\eta), \qquad \sigma_x^{(lf)}(x,\eta) = E_f\varepsilon_x^{(lf)}(x,\eta),$$
(2.7)
$$\tau_{xy}^{(uf)}(x,\eta) = \tau_{xy}^{(lf)}(x,\eta) = 0,$$

  where E_f is Young's modulus of the faces,
- the core

(2.8)
$$\sigma_x^{(c)}(x,\eta) = E_c\varepsilon_x^{(c)}(x,\eta), \qquad \tau_{xy}^{(c)}(x,\eta) = \frac{E_c}{2(1+\nu_c)}\gamma_{xy}^{(c)}(x,\eta),$$

  where E_c, ν_c are Young's modulus and Poisson's ratio of the core, respectively.

The bending moment is

(2.9)
$$M_b(x) = bh^2\left\{\int\limits_{-1/2}^{-\chi_c/2}\eta\sigma_x^{(uf)}(x,\eta)\,\mathrm{d}\eta + \int\limits_{-\chi_c/2}^{\chi_c/2}\eta\sigma_x^{(c)}(x,\eta)\,\mathrm{d}\eta + \int\limits_{\chi_c/2}^{1/2}\eta\sigma_x^{(lf)}(x,\eta)\,\mathrm{d}\eta\right\}.$$

Substituting expressions (2.7) and (2.8) for normal stresses and integrating, one obtains the following equation:

(2.10)
$$C_{vv}\frac{\mathrm{d}^2 v}{\mathrm{d}x^2} - C_{v\psi}\frac{\mathrm{d}\psi_f}{\mathrm{d}x} = -12\frac{M_b(x)}{E_f bh^3},$$

where $C_{vv} = 1-(1-e_c)\chi_c^3$, $C_{v\psi} = 3-(3-2e_c)\chi_c^2$, and $e_c = E_c/E_f$ are dimensionless coefficients.

The elastic strain energy of the beam is

$$U_\varepsilon = \frac{E_f bh}{2} \int_0^L \left[\Phi^{(uf)}(x) + e_c \Phi^{(c)}(x) + \Phi^{(uf)}(x)\right] \mathrm{d}x, \tag{2.11}$$

where

$$\Phi^{(uf)}(x) = \int_{-1/2}^{-\chi_c/2} \left[\varepsilon_x^{(uf)}(x,\eta)\right]^2 \mathrm{d}\eta,$$

$$\Phi^{(c)}(x) = \int_{-\chi_c/2}^{\chi_c/2} \left\{ \left[\varepsilon_x^{(c)}(x,\eta)\right]^2 + \frac{1}{2(1+\nu_c)} \left[\gamma_{xy}^{(c)}(x)\right]^2 \right\} \mathrm{d}\eta,$$

$$\Phi^{(lf)}(x) = \int_{\chi_c/2}^{1/2} \left[\varepsilon_x^{(lf)}(x,\eta)\right]^2 \mathrm{d}\eta.$$

Substituting expressions (2.4), (2.5), and (2.6) for strains into the above expression (2.11) and integrating, one obtains

$$U_\varepsilon = \frac{E_f bh^3}{24} \int_0^L \left\{ C_{vv} \left(\frac{\mathrm{d}^2 v}{\mathrm{d}x^2}\right)^2 - 2C_{v\psi} \frac{\mathrm{d}^2 v}{\mathrm{d}x^2} \frac{\mathrm{d}\psi_f}{\mathrm{d}x} + C_{\psi\psi} \left(\frac{\mathrm{d}\psi_f}{\mathrm{d}x}\right)^2 + C_\psi \frac{\psi_f^2(x,t)}{h^2} \right\} \mathrm{d}x, \tag{2.12}$$

where $C_{\psi\psi} = 4\,[3 - (3 - e_c)\chi_c]$, $C_\psi = \frac{24}{1+\nu_c} \frac{e_c}{\chi_c}$ are dimensionless coefficients.

The work of the load is

$$W = q \int_0^L v(x)\,\mathrm{d}x. \tag{2.13}$$

Therefore, based on the principle of stationary total potential energy $\delta(U_\varepsilon - W) = 0$, two differential equations of equilibrium of the classical sandwich beam are obtained in the following form:

$$C_{vv} \frac{\mathrm{d}^4 v}{\mathrm{d}x^4} - C_{v\psi} \frac{\mathrm{d}^3 \psi_f}{\mathrm{d}x^3} = 12 \frac{q}{E_f bh^3}, \tag{2.14}$$

$$C_{v\psi} \frac{\mathrm{d}^3 v}{\mathrm{d}x^3} - C_{\psi\psi} \frac{\mathrm{d}^2 \psi_f}{\mathrm{d}x^2} + C_\psi \frac{\psi_f(x)}{h^2} = 0. \tag{2.15}$$

It may be easily noticed that equations of fourth-order (2.14) and second-order (2.10) are equivalent. Thus, Eqs. (2.10) and (2.15) are governing equilibrium equations of the bending sandwich beams.

The scheme of the cut part of the beam with the load and reactions is shown in Fig. 3.

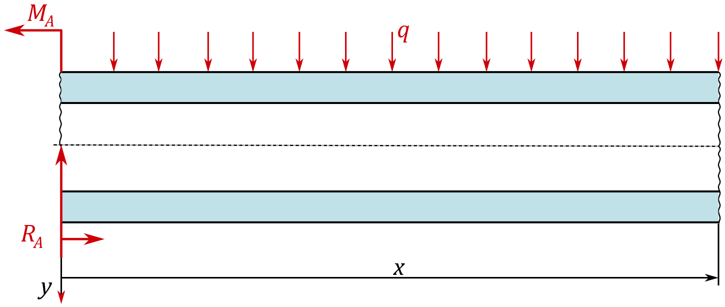

FIG. 3. Scheme of the cut part of the beam with the load and reactions.

The bending moment in accordance with the above scheme is as follows:

$$M_b(x) = R_A x - \frac{1}{2} q x^2 - M_0, \tag{2.16}$$

where $R_A = \frac{1}{2} qL$ is the reaction, and M_0 is the unknown reactive moment.

Consequently

$$M_b(x) = \frac{1}{2}\left(Lx - x^2\right) q - M_0. \tag{2.17}$$

The equilibrium Eqs. (2.10) and (2.15) apply to the classical sandwich beam with constant layers thicknesses. One can notice that the layers' thickness of the successive parts of the stepped beams (Fig. 1) are constant. Therefore, these equations with consideration of the expression (2.17) in the dimensionless coordinate ξ, are thus used in the analytical study of the stepped beam in the following form:

$$C_{vvi} \frac{\mathrm{d}^2 \overline{v}^{(i)}}{\mathrm{d}\xi^2} - C_{v\psi i} \frac{\mathrm{d}\psi_f^{(i)}}{\mathrm{d}\xi} = -6\left[\left(\xi - \xi^2\right) qL^2 - 2M_0\right] \frac{\lambda}{E_f b h^2}, \tag{2.18}$$

$$C_{v\psi i} \frac{\mathrm{d}^3 \overline{v}^{(i)}}{\mathrm{d}\xi^3} - C_{\psi\psi i} \frac{\mathrm{d}^2 \psi_f^{(i)}}{\mathrm{d}\xi^2} + C_{\psi i} \lambda^2 \psi_f^{(i)}(\xi) = 0, \tag{2.19}$$

where $\xi = x/L$ is the dimensionless coordinate, $\overline{v}^{(i)}(\xi) = v^{(i)}(\xi)/L$ is the relative deflection, $\lambda = L/h$ is the relative length of the beam, $i = 1, 2$ is the number of the beam part, and $C_{vvi} = 1 - (1 - e_c)\chi_{ci}^3$, $C_{v\psi i} = 3 - (3 - 2e_c)\chi_{ci}^2$, $C_{\psi\psi i} = 4\,[3 - (3 - e_c)\chi_{ci}]$, $C_{\psi i} = \frac{24}{1+\nu_c}\frac{e_c}{\chi_{ci}}$ are dimensionless coefficients.

This system, after simple transformation, is reduced to one differential equation in the form:

$$\text{(2.20)} \qquad \frac{\mathrm{d}^2\psi_f^{(i)}}{\mathrm{d}\xi^2} - (\alpha_i\lambda)^2\,\psi_f^{(i)}(\xi) = -6\,(1 - 2\xi)\,\frac{C_{v\psi i}}{C_{vvi}C_{\psi\psi i} - C_{v\psi i}^2}\lambda^3\frac{q}{E_f b},$$

here $\alpha_i = \sqrt{\frac{C_{v\psi i}C_{\psi i}}{C_{vvi}C_{\psi\psi i} - C_{v\psi i}^2}}$ – dimensionless coefficient.

The solution of this equation is the function – dimensionless displacement:

$$\text{(2.21)} \qquad \psi_f^{(i)}(\xi) = k_{c1}\,[C_{1i}\sinh(\alpha_i\lambda\xi) + C_{2i}\cosh(\alpha_i\lambda\xi) + 6\,(1 - 2\xi)]\,\lambda\frac{q}{E_f b},$$

where C_{1i}, C_{2i} are integration constants, and $k_{ci} = \frac{C_{v\psi i}}{C_{vvi}C_{\psi i}}$ is coefficient.

The function (2.21) for the individual parts of the stepped sandwich beam are as follows:

1) The first part of the beam ($0 \le \xi \le 1/3$), ($i = 1$) (Fig. 1): the condition: for $\xi = 0$, $\psi_f^{(1)}(0) = 0$, from which the constant $C_{21} = -6$, therefore

$$\text{(2.22)} \quad \psi_f^{(1)}(\xi) = k_{c1}\,[C_{11}\sinh(\alpha_1\lambda\xi) - 6\cosh(\alpha_1\lambda\xi) + 6\,(1 - 2\xi)]\,\lambda\frac{q}{E_f b}.$$

The value of this function for $\xi = 1/3$ is as follows:

$$\text{(2.23)} \qquad \psi_f^{(1)}\left(\frac{1}{3}\right) = k_{c1}\,[C_{11}\sinh(\alpha_1\lambda/3) - 6\cosh(\alpha_1\lambda/3) + 2]\,\lambda\frac{q}{E_f b}.$$

2) The second-middle part of the beam ($1/3 \le \xi \le 1/2$), ($i = 2$) (Fig. 1): the condition: for $\xi = 1/2$, $\psi_f^{(1)}\left(\frac{1}{2}\right) = 0$, from which the constant $C_{22} = -C_{12}\tanh(\alpha_2\lambda/2)$, therefore

$$\text{(2.24)} \qquad \psi_f^{(2)}(\xi) = k_{c2}\left\{C_{12}\frac{\sinh[\alpha_2\lambda\,(\xi - 1/2)]}{\cosh(\alpha_2\lambda/2)} + 6(1 - 2\xi)\right\}\lambda\frac{q}{E_f b}.$$

The value of the nonlinear component of this function is negligibly small – almost zero. Therefore, this function is linear in the following form:

$$\text{(2.25)} \qquad \psi_f^{(2)}(\xi) = 6k_{c2}(1 - 2\xi)\lambda\frac{q}{E_f b}.$$

The value of this function for $\xi = 1/3$ is as follows:

$$\text{(2.26)} \qquad \psi_f^{(2)}\left(\frac{1}{3}\right) = 2k_{c2}\lambda\frac{q}{E_f b}.$$

Based on the consistency condition for displacements $\psi_f^{(1)}(1/3) = \psi_f^{(2)}(1/3)$, with consideration of the expressions (2.23) and (2.26), one obtains the integration constant

$$C_{11} = 6\frac{\cosh(\alpha_1\lambda/3)}{\sinh(\alpha_1\lambda/3)} + 2\frac{1}{\sinh(\alpha_1\lambda/3)}\left(\frac{k_{c2}}{k_{c1}} - 1\right). \tag{2.27}$$

Consequently, the dimensionless displacement function (2.22) is as follows:

$$\psi_f^{(1)}(\xi) = k_{c1}\left\{-6\frac{\sinh[\alpha_1\lambda(1/3-\xi)]}{\sinh(\alpha_1\lambda/3)} + 2\frac{\sinh(\alpha_1\lambda\xi)}{\sinh(\alpha_1\lambda/3)}\left(\frac{k_{c2}}{k_{c1}} - 1\right) + 6(1-2\xi)\right\}\lambda\frac{q}{E_f b}. \tag{2.28}$$

Equation (2.18) after the first integration for the individual parts of the stepped sandwich beam is as follows:

1) The first part of the beam $(0 \le \xi \le 1/3)$, $(i = 1)$ (Fig. 1)

$$C_{vv1}\frac{d\overline{v}^{(1)}}{d\xi} = C_{31} + C_{v\psi 1}\psi_f^{(1)}(\xi) - 6\left[\left(\frac{1}{2}\xi^2 - \frac{1}{3}\xi^3\right)qL^2 - 2\xi M_0\right]\frac{\lambda}{E_f b h^2}. \tag{2.29}$$

The conditions: for $\xi = 0$, $\left.\frac{d\overline{v}^{(1)}}{d\xi}\right|_0 = 0$, and $\psi_f^{(1)}(0) = 0$, from which the constant $C_{31} = 0$, therefore

$$C_{vv1}\frac{d\overline{v}^{(1)}}{d\xi} = C_{v\psi 1}\psi_f^{(1)}(\xi) - 6\left[\left(\frac{1}{2}\xi^2 - \frac{1}{3}\xi^3\right)qL^2 - 2\xi M_0\right]\frac{\lambda}{E_f b h^2}. \tag{2.30}$$

The value of this function for $\xi = 1/3$ is as follows:

$$\left.\frac{d\overline{v}^{(1)}}{d\xi}\right|_{1/3} = \left[2k_{c2}C_{v\psi 1}q - \left(\frac{7}{27}qL^2 - 4M_0\right)\frac{1}{h^2}\right]\frac{1}{C_{vv1}}\frac{\lambda}{E_f b}. \tag{2.31}$$

Integrating Eq. (2.30) with consideration of the function (2.28), one obtains

$$\overline{v}^{(1)}(\xi) = \frac{C_{41}}{C_{vv1}} + \left\{2k_{c1}C_{v\psi 1}\Phi_f^{(1)}(\xi)q - \left[\left(\xi^3 - \frac{1}{2}\xi^4\right)qL^2 - 6\xi^2 M_0\right]\frac{1}{h^2}\right\}\frac{1}{C_{vv1}}\frac{\lambda}{E_f b}, \tag{2.32}$$

where

$$\Phi_f^{(1)}(\xi) = \frac{3\cosh\left[\alpha_1\lambda(1/3-\xi)\right] + (k_{c2}/k_{c1}-1)\cosh\left(\alpha_1\lambda\xi\right)}{\alpha_1\lambda\sinh\left(\alpha_1\lambda/3\right)} + 3(\xi-\xi^2).$$

The condition: for $\xi = 0$, $\overline{v}^{(1)}(0) = 0$, from which the constant

$$C_{41} = -2C_{v\psi 1}\frac{3k_{c1}\cosh\left(\alpha_1\lambda/3\right) - k_{c1} + k_{c2}}{\alpha_1\lambda\sinh\left(\alpha_1\lambda/3\right)}\lambda\frac{q}{E_f b}. \tag{2.33}$$

The value of this function (2.32) for $\xi = 1/3$ is as follows:

$$\overline{v}^{(1)}\left(\frac{1}{3}\right) = \left\{2C_{v\psi 1}\left[\frac{2}{3}k_{c1} - (4k_{c1}-k_{c2})\frac{\cosh\left(\alpha_1\lambda/3\right)-1}{\alpha_1\lambda\sinh\left(\alpha_1\lambda/3\right)}\right]q - \frac{1}{3}\left(\frac{5}{54}qL^2 - 2M_0\right)\frac{1}{h^2}\right\}\frac{1}{C_{vv1}}\frac{\lambda}{E_f b}. \tag{2.34}$$

2) The second-middle part of the beam $(1/3 \le \xi \le 1/2)$, $(i = 2)$ (Fig. 1)

$$C_{vv2}\frac{d\overline{v}^{(2)}}{d\xi} = C_{32} + C_{v\psi 2}\psi_f^{(2)}(\xi) - 6\left[\left(\frac{1}{2}\xi^2 - \frac{1}{3}\xi^3\right)qL^2 - 2\xi M_0\right]\frac{\lambda}{E_f b h^2}, \tag{2.35}$$

The conditions: for $\xi = 1/2$, $\left.\frac{d\overline{v}^{(2)}}{d\xi}\right|_{1/2} = 0$, and $\psi_f^{(2)}(1/2) = 0$, from which the constant $C_{32} = \frac{1}{2}\left(qL^2 - 12M_0\right)\frac{\lambda}{E_f b h^2}$, therefore

$$\frac{d\overline{v}^{(2)}}{d\xi} = \left\{6k_{c2}C_{v\psi 2}\left(1-2\xi\right)q + \left[\left(\frac{1}{2} - 3\xi^2 + 2\xi^3\right)qL^2 + 6\left(2\xi-1\right)M_0\right]\frac{1}{h^2}\right\}\frac{1}{C_{vv2}}\frac{\lambda}{E_f b}. \tag{2.36}$$

The value of this function for $\xi = 1/3$ is as follows:

$$\left.\frac{d\overline{v}^{(2)}}{d\xi}\right|_{1/3} = \left[2k_{c2}C_{v\psi 2}q + \left(\frac{13}{54}qL^2 - 2M_0\right)\frac{1}{h^2}\right]\frac{1}{C_{vv2}}\frac{\lambda}{E_f b}. \tag{2.37}$$

Integrating Eq. (2.36), one obtains

$$\overline{v}^{(2)}(\xi) = C_{42} + \left\{6k_{c2}C_{v\psi 2}(\xi-\xi^2)q + \left[\left(\frac{1}{2}\xi - \xi^3 + \frac{1}{2}\xi^4\right)qL^2 + 6\left(\xi^2-\xi\right)M_0\right]\frac{1}{h^2}\right\}\frac{1}{C_{vv2}}\frac{\lambda}{E_f b}. \tag{2.38}$$

The value of this function (2.38) for $\xi = 1/3$ is as follows:

$$(2.39)\qquad \overline{v}^{(2)}\left(\frac{1}{3}\right) = C_{42} + \left\{\frac{4}{3}k_{c2}C_{v\psi 2}q + \frac{1}{3}\left(\frac{11}{27}qL^2 - 4M_0\right)\frac{1}{h^2}\right\}\frac{1}{C_{vv2}}\frac{\lambda}{E_f b}.$$

Based on the consistency condition for the slope of the deflection curve $\left.\frac{\mathrm{d}\overline{v}^{(1)}}{\mathrm{d}\xi}\right|_{1/3} = \left.\frac{\mathrm{d}\overline{v}^{(2)}}{\mathrm{d}\xi}\right|_{1/3}$, with consideration of the expressions (2.31) and (2.37), one obtains the reactive moment

$$(2.40)\qquad M_0 = \overline{M}_0 qL^2,$$

where

$$(2.41)\qquad \overline{M}_0 = \frac{(13C_{vv1} + 14C_{vv2})\,\lambda^2 + 108k_{c2}\,(C_{vv1}C_{v\psi 2} - C_{vv2}C_{v\psi 1})}{108\,(C_{vv1} + 2C_{vv2})\,\lambda^2}.$$

Based on the consistency condition for the deflection $\overline{v}^{(1)}\left(\frac{1}{3}\right) = \overline{v}^{(2)}\left(\frac{1}{3}\right)$, with consideration of the expressions (2.34), (2.39), and (2.40), one obtains the constant

$$(2.42)\qquad C_{42} = \left\{2\frac{C_{vv1}}{C_{vv1}}\left[\frac{2}{3}k_{c1} - (4k_{c1} - k_{c2})\frac{\cosh(\alpha_1\lambda/3) - 1}{\alpha_1\lambda\sinh(\alpha_1\lambda/3)}\right] - \frac{4}{3}k_{c2}\frac{C_{v\psi 2}}{C_{vv2}} - \frac{1}{3}\left[\left(\frac{5}{54} - 2\overline{M}_0\right)\frac{1}{C_{vv1}} + \left(\frac{11}{27} - 4\overline{M}_0\right)\frac{1}{C_{vv2}}\right]\lambda^2\right\}\lambda\frac{q}{E_f b}.$$

Taking into account expression (2.38) with consideration of expressions (2.40) and (2.42), after simple transformation, the maximum deflection of the beam is in the following form:

$$(2.43)\qquad \overline{v}_{\max}^{(\mathrm{An})} = \overline{v}^{(2)}\left(\frac{1}{2}\right) = \widetilde{v}_{\max}^{(\mathrm{An})}\frac{q}{E_f b},$$

where the dimensionless maximum deflection of the beam is

$$(2.44)\qquad \widetilde{v}_{\max}^{(\mathrm{An})} = k_{v0}\lambda^3 + k_{vse}\lambda,$$

and the coefficient of the dimensionless deflection of the pure bending is

$$(2.45)\qquad k_{v0} = \frac{1}{6}\left[\left(\frac{53}{432} - \overline{M}_0\right)\frac{1}{C_{vv2}} - \left(\frac{5}{27} - 4\overline{M}_0\right)\frac{1}{C_{vv1}}\right],$$

and the coefficient of the dimensionless deflection of the shear effect is

$$(2.46)\qquad k_{vse} = \frac{1}{6}\left(8k_{c1}\frac{C_{v\psi 1}}{C_{vv1}} + k_{c2}\frac{C_{v\psi 2}}{C_{vv2}}\right) - 2\,(4k_{c1} - k_{c2})\frac{\cosh(\alpha_1\lambda/3) - 1}{\alpha_1\lambda\sinh(\alpha_1\lambda/3)}\frac{C_{v\psi 1}}{C_{vv1}}.$$

Thus, the dimensionless maximum deflection of the beam (2.44), after simple transformation, is as follows:

$$\tilde{v}_{\max}^{(\mathrm{An})} = (1 + C_{se})\, k_{v0}\lambda^3, \tag{2.47}$$

where the coefficient of the shear effect

$$C_{se} = \frac{k_{vse}}{k_{v0}\lambda^2}. \tag{2.48}$$

The detailed calculations of the exemplary stepped sandwich beams with a constant volume of the core and faces are carried out for the following data: the relative length $\lambda = 20$, dimensionless coefficient of Young's modules $e_c = 1/20$, Poisson's ratio of the core $\nu_c = 0.3$.

Example 1. The relative core thickness sum $2\chi_{c1} + \chi_{c2} = 51/20$. The results of the calculations are specified in Table 1.

Table 1. Values of the shear effect coefficient (2.45) and the dimensionless maximum deflection (2.44).

χ_{c1}	16.5/20	17.0/20	17.28/20	17.5/20	18.0/20
χ_{c2}	18.0/20	17.0/20	16.44/20	16.0/20	15.0/20
C_{se}	0.2020	0.2142	0.2165	0.2161	0.2081
$\tilde{v}_{\max}^{(\mathrm{An})}$	760.02	728.66	724.48	727.05	752.60

The diagram of the dimensionless maximum deflection (2.47), being a function of the relative core thickness χ_{c1} of the first part of the beam, is shown in Fig. 4.

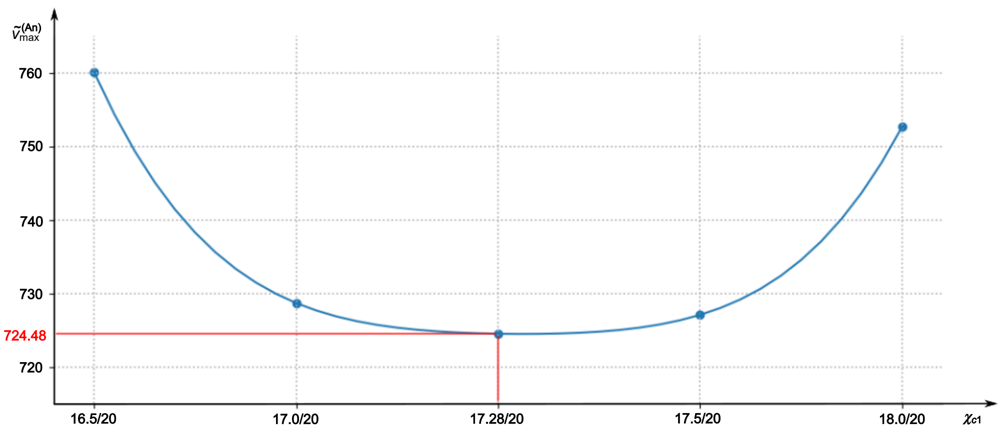

FIG. 4. Diagram of the dimensionless maximum deflection $\tilde{v}_{\max}^{(\mathrm{An})}(\chi_{c1})$ – *Example 1.*

The minimum value of the maximum dimensionless deflection of this stepped sandwich beam is for the structure case of the relative thicknesses $\chi_{c1} = 17.28/20$ and $\chi_{c2} = 16.44/20$. Therefore, for this structure case, the bending beam rigidity is maximum.

Example 2. The relative core thickness sum $2\chi_{c1} + \chi_{c2} = 48/20$. The results of the calculations are specified in Table 2.

Table 2. Values of the shear effect coefficient (2.45) and the dimensionless maximum deflection (2.44).

χ_{c1}	15.5/20	16.0/20	16.31/20	16.5/20	17.0/20
χ_{c2}	17.0/20	16.0/20	15.38/20	15.0/20	14.0/20
C_{se}	0.2490	0.2596	0.2623	0.2626	0.2584
$\tilde{v}_{\max}^{(\mathrm{An})}$	628.95	613.14	610.67	611.59	622.65

The diagram of the dimensionless maximum deflection (2.47), being a function of the relative core thickness χ_{c1} of the first part of the beam, is shown in Fig. 5.

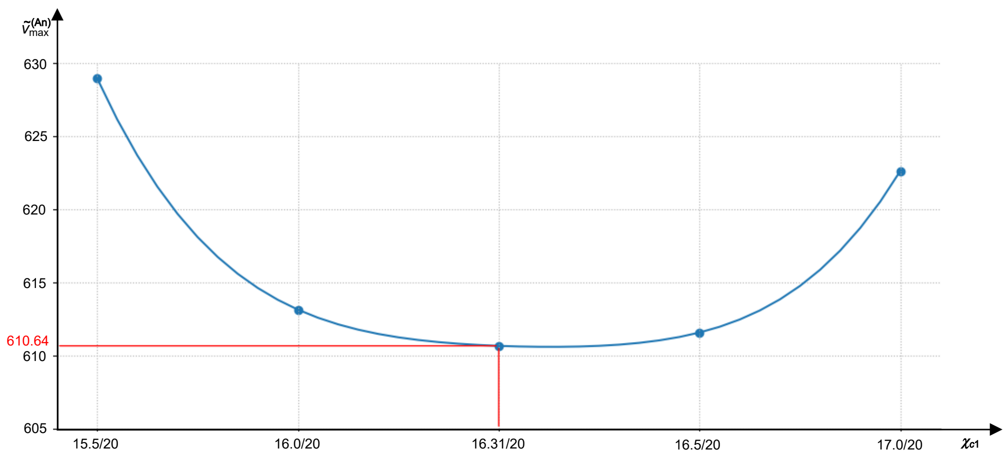

FIG. 5. Diagram of the dimensionless maximum deflection $\tilde{v}_{\max}^{(\mathrm{An})}(\chi_{c1})$ – *Example 2.*

The minimum value of the maximum dimensionless deflection of this stepped sandwich beam is for the structure case of relative thicknesses $\chi_{c1} = 16.31/20$ and $\chi_{c2} = 15.38/20$. Therefore, for this structure case, the bending beam rigidity is maximum.

3. Numerical-FEM model and calculations

The numerical model of the beam is elaborated for comparison with the analytical results. Computational calculations are conducted in Abaqus software. The model and mesh of the exemplary beam are shown in Fig. 6.

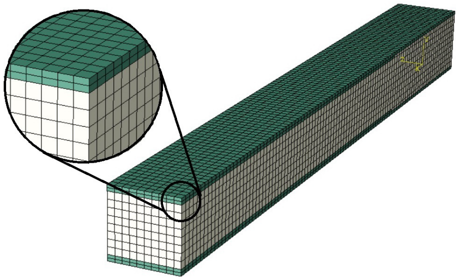

Fig. 6. Numerical FEM model of the exemplary beams-element mesh (Abaqus 6.12).

The computational model of the beam is a solid consisting of three layers, which is placed in the Cartesian coordinate system. The longitudinal x-axis is collinear with the beam neutral axis, the y-axis is directed upward, and z-axis is perpendicular to the beam neutral axis. Due to the symmetry of the beam, only half of it is considered. The beam is under a continuous load and its ends are clamped. To reach that, appropriate boundary conditions are imposed:

- the displacement vector component perpendicular to the symmetry plane is zero,
- the rotational vector components parallel to the symmetry plane are zero,
- the displacement and rotational vector components are zero in clamped ends.

The mesh of the numerical model consists of 10 000 quadratic hexahedral finite elements (C3D8R type) and 12 221 nodes.

The FEM calculations of the exemplary stepped sandwich beams are carried out for the following data: sizes $L = 400$ mm, $h = 20$ mm, $b = 20$ mm, $q = 1.0$ N/mm, material constants $E_f = 72000$ MPa, $E_c = 3600$ MPa, $\nu_c = 0.3$, thus $\lambda = 20$, $e_c = 1/20$, and other data are adopted the same as in the analytical studies. The results of the calculations are specified in Tables 3 and 4.

Table 3. Values of the maximum deflection – FEM – *Example 1*.

χ_{c1} χ_{c2}	16.5/20 18.0/20	17.0/20 17.0/20	17.28/20 16.44/20	17.5/20 16.0/20	18.0/20 15.0/20
$\overline{v}_{\max}^{(\mathrm{FEM})}$	4.202	4.052	4.029	4.046	4.196
$\widetilde{v}_{\max}^{(\mathrm{FEM})}$	756.36	729.36	725.22	728.28	755.28

The differences between analytical (An) and numerical (FEM) results are below 0.48% in these exemplary stepped sandwich beams.

Table 4. Values of the maximum deflection – FEM – *Example 2*.

χ_{c1} χ_{c2}	15.5/20 17.0/20	16.0/20 16.0/20	16.31/20 15.38/20	16.5/20 15.0/20	17.0/20 14.0/20
$\overline{v}_{\max}^{(\mathrm{FEM})}$	3.490	3.424	3.407	3.414	3.482
$\widetilde{v}_{\max}^{(\mathrm{FEM})}$	628.20	616.32	613.26	614.52	626.78

The differences between analytical (An) and numerical (FEM) results are below 0.66% in these exemplary stepped sandwich beams.

4. Final remarks

In this article, the analytical model of the sandwich stepped beam with clamped ends was considered. This model was developed on the basis of the "broken-line" hypothesis. The focus was placed on the shear effect during the bending of the beam.

The analytical studies have shown a significant influence of the shear effect on the deflection of sandwich beams with clamped ends. The values of the shear effect coefficient C_{se}, present in expression (2.44), determined for the example beams (Tables 1 and 2), are in the range (0.202–0.217) and (0.249–0.263). Thus, the share of the shear effect in the deflection of the example beams is greater than 20%.

An equivalent computational model was developed to make FEM calculations for the same beams. The Abaqus software was used both for modeling and calculating. The purpose of the FEM calculations was to compare with the analytical results. The beam deflection values determined with the two methods differ slightly, and this difference does not exceed 0.31%.

References

1. Birman V., Kardomateas G.A., Review of current trends in research and applications of sandwich structures, *Composites Part B*, **142**: 221–240, 2018, doi: 10.1016/j.compositesb.2018.01.027.

2. Carrera E., Brischetto S., A survey with numerical assessment of classical and refined theories for the analysis of sandwich plates, *Applied Mechanics Reviews*, **62**(1): 010803, 2009, doi: 10.1115/1.3013824.

3. Chinh T.H., Tu T.M., Duc D.M., Hung T.Q., Static flexural analysis of sandwich beam with functionally graded face sheets and porous core via point interpolation meshfree

method based on polynomial basic function, *Archive of Applied Mechanics*, **91**(3): 933–947, 2021, doi: 10.1007/s00419-020-01797-x.

4. Draiche K., Bousahla A.A., Tounsi A., Hussain M., An integral shear and normal deformation theory for bending analysis of functionally graded sandwich curved beams, *Archive of Applied Mechanics*, **91**(12): 4669–4691, 2021, doi: 10.1007/s00419-021-02005-0.

5. Icardi U., Applications of zig-zag theories to sandwich beams, *Mechanics of Advanced Materials and Structures*, **10**(1): 77–97, 2003, doi: 10.1080/15376490306737.

6. Kreja I., A literature review on computational models for laminated composite and sandwich panels, *Central European Journal of Engineering*, **1**(1): 59–80, 2011, doi: 10.2478/s13531-011-0005-x.

7. Magnucka-Blandzi E., Magnucki K., Effective design of a sandwich beam with a metal foam core, *Thin-Walled Structures*, **45**(4): 432–438, 2007, doi: 10.1016/j.tws.2007.03.005.

8. Magnucka-Blandzi E., Bending and buckling of a metal seven-layer beam with crosswise corrugated main core – Comparative analysis with sandwich beam, *Composite Structures*, **183**: 35–41, 2018, doi: 10.1016/j.compstruct.2016.11.089.

9. Magnucki K., Jasion P., Szyc W., Smyczynski M., Strength and buckling of a sandwich beam with thin binding layers between faces and a metal foam core, *Steel and Composite Structures*, **16**(3): 325–337, 2014, doi: 10.12989/scs.2014.16.3.325.

10. Magnucki K., Magnucka-Blandzi E., Lewiński J., Milecki S., Analytical and numerical studies of an unsymmetrical sandwich beam – bending, buckling and free vibration, *Engineering Transactions*, **67**(4): 491–512, 2019, doi: 10.24423/EngTrans.1015.20190725.

11. Magnucki K., Bending of symmetrically sandwich beams and I-beams – Analytical study, *International Journal of Mechanical Sciences*, **150**: 411–419, 2019, doi: 10.1016/j.ijmecsci.2018.10.020.

12. Magnucki K., Magnucka-Blandzi E., Generalization of a sandwich structure model: Analytical studies of bending and buckling problems of rectangular plates, *Composite Structures*, **255**: 112944, 2021, doi: 10.1016/j.compstruct.2020.112944.

13. Magnucki K., Magnucka-Blandzi E., Wittenbeck L., Three models of a sandwich beam: Bending, buckling and free vibration, *Engineering Transactions*, **70**(2): 97–122, 2022, doi: 10.24423/EngTrans.1416.20220331.

14. Nguyen C.H., Chandrashekhara K., Birman V., Enhanced static response of sandwich panel with honeycomb cores through the use of stepped facings, *Journal of Sandwich Structures and Materials*, **13**(2): 237–260, 2011, doi: 10.1177/1099636210369615.

15. Noor A.K, Burton W.S., Bert C.W., Computational models for sandwich panels and shells, *Applied Mechanics Reviews*, **49**(3): 155–199, 1996, doi: 10.1115/1.3101923.

16. Phan C.N., Frostig Y., Kardomateas G.A., Analysis of sandwich beams with a compliant core and with in-plane rigidity–extended high-order sandwich panel theory versus elasticity, *ASME: Journal of Applied Mechanics*, **79**(4): 041001-1–11, 2012, doi: 10.1115/1.4005550.

17. Sayyad A.S., Ghugal Y.M., Bending, buckling and free vibration of laminated composite and sandwich beams: a critical review of literature, *Composite Structures*, **171**: 486–504, 2017, doi: 10.1016/j.compstruct.2017.03.053.

18. Sayyad A.S., Ghugal Y.M., Modeling and analysis of functionally graded sandwich beams: A review, *Mechanics of Advanced Materials and Structures*, **26**(21): 1776–1795, 2019, doi: 10.1080/15376494.2018.1447178.

Received May 25, 2022; accepted version November 8, 2022.